



Cite this: DOI: 10.1039/d6cb00061d

# Backbone N-heteroatom substitution as a strategy to enhance peptide proteolytic stability

Avraz F. Anwar, Natalia Cano-Sampaio and Juan R. Del Valle \*

Peptide-based ligands are well-suited to engage large biomolecular surfaces but are often limited by rapid proteolytic degradation in biological environments. Backbone modification offers a direct means to disrupt protease recognition while preserving side chain functionality; however, many established approaches impose conformational constraints that compromise biological activity. Here, we evaluate backbone *N*-amino and *N*-hydroxy substitution as a strategy for enhancing peptide proteolytic stability. Using a defined chymotrypsin substrate, we demonstrate that backbone *N*-amination confers pronounced, position-dependent protection when introduced at or adjacent to the scissile bond. Extending these findings to a  $\beta$ -sheet-forming antimicrobial peptide, we show that poly-*N*-amination dramatically enhances serum stability while preserving or enhancing conformation-dependent antibacterial activity. Together, these results expand the repertoire of peptide backbone modifications that mitigate proteolytic degradation while retaining the conformational and functional features required for the design of peptide- and protein-based biological probes.

Received 12th February 2026,  
Accepted 20th April 2026

DOI: 10.1039/d6cb00061d

rsc.li/rsc-chembio

## Introduction

Peptides represent a chemically versatile platform for engaging expansive and shallow biomolecular surfaces that are difficult to target with small molecules.<sup>1,2</sup> However, their use in cellular and *in vivo* studies is often undermined by rapid proteolytic degradation. Endogenous proteases efficiently process canonical  $\alpha$ -peptide backbones, which generally adopt  $\beta$ -strand-like local conformation prior to enzymatic cleavage.<sup>3</sup> The short lifetime of peptides in tissue and serum thus poses a major obstacle to their development as chemical probes and therapeutics.<sup>4,5</sup>

Numerous chemical strategies have been developed to address the problem of peptide proteolysis, including main chain macrocyclization, the incorporation of noncanonical residues, and backbone amide substitution (Fig. 1).<sup>6–11</sup> Amide *N*-methylation has emerged as an extensively studied modification, with previous work demonstrating strong positional effects on proteolytic susceptibility that arise from disruption of hydrogen-bonding interactions required for protease binding.<sup>8,12–14</sup> However, *N*-methylation and related approaches can impose conformational constraints that compromise biological activity.<sup>15–17</sup> This trade-off is particularly problematic for peptides whose function depends on extended backbone conformations that are predisposed to interact with proteases.<sup>3</sup> There remains a need for additional backbone editing

approaches that can inform the design of conformationally and proteolytically stable peptidomimetics.

Hydrazide and hydroxamate bonds differ fundamentally from amides in their electronic properties, hydrogen-bonding behavior, and conformational bias. Recent studies from our laboratory have shown that backbone *N*-amination and *N*-hydroxylation can stabilize  $\beta$ -sheet conformations through cooperative noncovalent interactions, suggesting that *N*-heteroatom substitution may offer a unique combination of conformational control and side chain preservation.<sup>18–21</sup> Despite considerable insights into the folding preferences of *N*-heteroatom-substituted peptides, the impact of these backbone modifications on proteolytic stability has not been systematically explored.<sup>22</sup>

### Backbone modifications that enhance proteolytic stability:

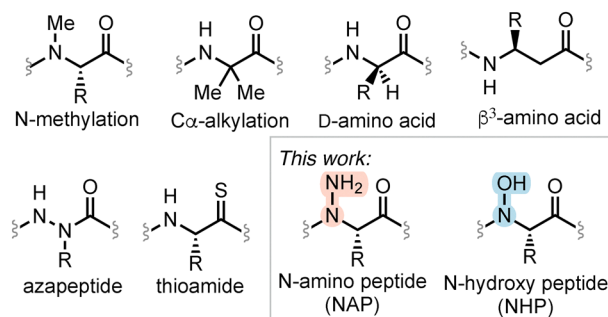


Fig. 1 Strategies to enhance peptide proteolytic stability through modifications to the backbone.

Department of Chemistry & Biochemistry, University of Notre Dame, Notre Dame, IN 46556, USA. E-mail: jdelvalle@nd.edu



In this study, we employ a chymotrypsin substrate sequence to investigate how backbone *N*-amino and *N*-hydroxy substitutions influence proteolytic stability as a function of position relative to the scissile bond. We then apply these insights to a  $\beta$ -sheet-forming antimicrobial peptide, demonstrating that poly-*N*-amination confers exceptional serum stability while preserving or enhancing conformation-dependent antibacterial activity. Together, these results establish backbone *N*-heteroatom substitution as a chemically distinct, minimalist strategy for stabilizing bioactive peptides.

## Results and discussion

To assess the proteolytic susceptibility of peptides featuring backbone *N*-heteroatom substituents, we employed a sequence variant of a model originally reported by Horne and co-workers (1, Fig. 2A).<sup>8</sup> Peptide 1 contains a single chymotrypsin cleavage site between Tyr (P1) and Lys (P1') and lacks any appreciable secondary structure (Fig. S1). This design enables direct evaluation of how a single backbone modification at or near the scissile bond influences the rate of proteolysis, independent of conformational effects that could otherwise complicate interpretation.

We synthesized a series of *N*-aminated substrates (2–7) in which a single residue in positions P3 through P3' was replaced with its corresponding  $\alpha$ -hydrazino acid. The *N*-amino peptides (NAPs) were prepared using our previously reported monomer-based synthetic strategy (Fig. 2B).<sup>23</sup> Briefly, zwitterionic amino acids were selectively aminated at the  $\alpha$ -nitrogen using the oxaziridine reagent TBDOT<sup>24</sup> to afford the corresponding  $\alpha$ -hydrazino acids. These monomers were incorporated into the peptide sequence *via* standard Fmoc solid-phase peptide synthesis (SPPS), with subsequent Boc hydrazide acylation achieved through acid chloride-mediated coupling. Following elongation and cleavage from the resin, all peptides were purified by RP-HPLC and characterized by HRMS and analytical HPLC (Table 1).

With peptides 1–7 in hand, their proteolytic stability was evaluated by incubation with chymotrypsin and quantification of intact peptide over time by analytical HPLC. For all peptides

**Table 1** Parent peptide (1) and NAP variants (2–7) prepared by SPPS, and half-lives ( $t_{1/2}$ ) in the presence of chymotrypsin (derived from non-linear regression of RP-HPLC-monitored degradation,  $n = 3$ ). aXaa = *N*-aminated ( $\alpha$ -hydrazino acid) residue

Peptide	P3	P2	P1	P1'	P2'	P3'	$t_{1/2}$ (min)
1	Ala	Ala	Tyr	Lys	Ser	Ala	2.0
2	aAla	Ala	Tyr	Lys	Ser	Ala	5.3
3	Ala	aAla	Tyr	Lys	Ser	Ala	3.5
4	Ala	Ala	aTyr	Lys	Ser	Ala	300
5	Ala	Ala	Tyr	aLys	Ser	Ala	202
6	Ala	Ala	Tyr	Lys	aSer	Ala	6.2
7	Ala	Ala	Tyr	Lys	Ser	aAla	2.5

examined, data was fit to a single-phase exponential decay model to derive relative half-lives (Fig. 3 and Fig. S2). Notably, peptides 4 and 5, bearing *N*-amino substituents immediately preceding (P1) and at the scissile bond (P1'), respectively, exhibited half-lives that were 100–150-fold greater than that of the unmodified control peptide 1. In contrast, peptides 2, 3, 6, and 7, which feature *N*-amino modifications more distal to the cleavage site, exhibited half-lives within one order of magnitude of peptide 1. This positional dependence is consistent with a prior study showing that backbone *N*-methylation confers the greatest protection when introduced at amides that would otherwise engage chymotrypsin as H-bond donors (P3, P1, P2').<sup>8</sup> These results establish the protective effect of *N*-amination at or near the chymotrypsin cleavage site. This effect likely arises from a combination of altered substrate binding, reduced acyl-enzyme formation, and local conformational

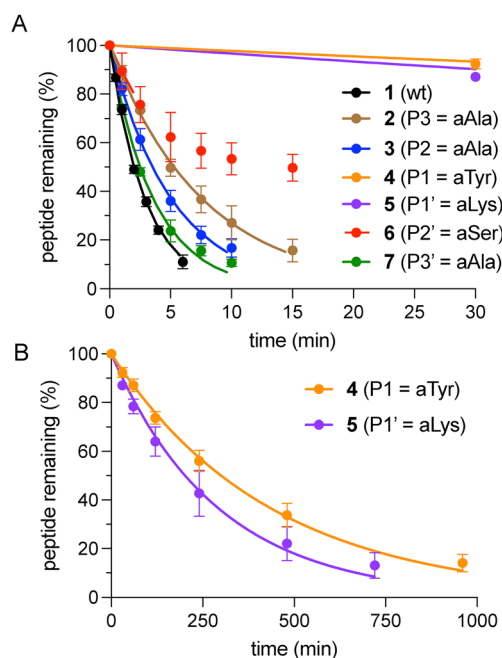


**Fig. 3** (A) Chymotrypsin-mediated degradation of 1–7 over 30 min, monitored by RP-HPLC ( $\lambda = 220$  nm). Curves are derived from non-linear regression and error bars represent SD for each data point ( $n = 3$ ). In the case of peptide 6, curve-fitting is based only on the initial 3 time points due to apparent chymotrypsin inactivation by the substrate.<sup>8</sup> (B) Extended time scale showing degradation of 4 and 5.

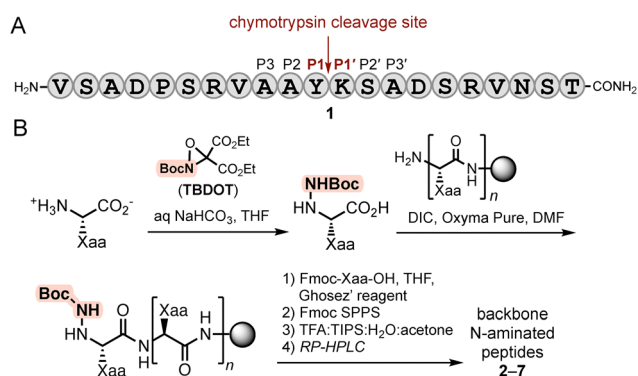


**Fig. 2** (A) Sequence and cleavage site of a model chymotrypsin substrate (1). (B) Synthesis of *N*-amino peptide variants of 1.



changes; however, the current data do not distinguish among these possibilities.

On the basis of these results, we sought to compare *N*-amination at P1 and P1' directly to *N*-hydroxylation and *N*-methylation using the same parent sequence. Our group recently reported the synthesis of *N*-hydroxy peptides (NHPs) *via* chemoselective ligation of thioesters with peptide segments featuring a hydroxamate at the penultimate residue.<sup>25</sup> We used this protocol to prepare **8** and **9**, which incorporate *N*-hydroxy Tyr (hTyr) at P1 or *N*-hydroxy Lys (hLys) at P1', respectively (Fig. 4). We also synthesized *N*-methyl peptides (NMPs) **10** and **11** by conventional SPPS for comparison (Table 2).

These peptides were evaluated using the same chymotrypsin stability assay described above (Fig. 5 and Fig. S2). Introduction of an *N*-hydroxy substituent at the P1 position (**8**) resulted in approximately 40-fold increase in proteolytic stability relative to **1**. Although this enhancement was lower than that observed for the corresponding *N*-amino (**4**) and *N*-methyl (**10**) peptides, it nonetheless demonstrates that backbone *N*-hydroxylation at P1 can significantly slow proteolysis. In contrast, hydroxamate substitution at the P1' position (**9**) resulted in only a modest increase in stability relative to **1**, with proteolysis occurring significantly faster than *N*-amino variant **5** or *N*-methyl variant **11**. Greater electrophilicity of the hydroxamate carbonyl at the scissile bond likely increases its susceptibility to hydrolysis relative to the hydrazide and tertiary amide variants, contributing to its weaker stabilization. Random coil CD signatures for each of the peptides tested (**1–11**) suggest that the observed stability trends are not the result of global conformational changes, although local perturbations, which are not distinguished in CD, may have an effect (Fig. S1).

While backbone amide substitution represents a convenient and effective strategy to enhance resistance to proteolysis, the potential for significant conformational perturbation can limit such strategies in the context of bioactive peptides. We thus sought to investigate whether *N*-amination could enhance the stability of a peptide whose biological activity depends on conformation. Toward this end, we selected a known  $\beta$ -sheet-forming antimicrobial peptide (AMP) composed of four

**Table 2** NHP and NMP peptide substrates prepared by SPPS, and half-lives ( $t_{1/2}$ ) in the presence of chymotrypsin (derived from non-linear regression of RP-HPLC-monitored degradation,  $n = 3$ ). hXaa = *N* $\alpha$ -hydroxy amino acid, MeXaa = *N* $\alpha$ -methyl amino acid

Peptide	P3	P2	P1	P1'	P2'	P3'	$t_{1/2}$ (min)
<b>8</b>	Ala	Ala	<b>hTyr</b>	Lys	Ser	Ala	83
<b>9</b>	Ala	Ala	Tyr	<b>hLys</b>	Ser	Ala	7.3
<b>10</b>	Ala	Ala	<b>MeTyr</b>	Lys	Ser	Ala	1311
<b>11</b>	Ala	Ala	Tyr	<b>MeLys</b>	Ser	Ala	832

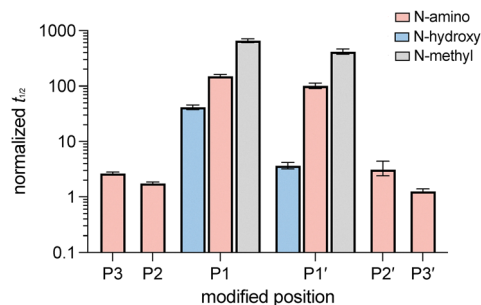


**Fig. 5** Relative chymotrypsin stabilities of peptides **2–11**. Half-lives derived from non-linear regression were normalized to that of parent (unmodified) peptide **1**. Error bars represent normalized 95% CI values from curve fitting.

repeating Ile-Lys dipeptides (**12**, Table 3).<sup>26,27</sup> Peptide **12** exhibits poor serum stability but possesses broad-spectrum anti-bacterial activity linked to its amphipathic  $\beta$ -sheet structure upon binding to the bacterial membrane. Our group previously showed that, in contrast to *N*-methylation, backbone *N*-amination of  $C\alpha$ -substituted amino acid residues can significantly increase the folded population of  $\beta$ -sheet model peptides.<sup>18,19</sup> We therefore hypothesized that *N*-amination

**Table 3** H-[Ile-Lys]<sub>4</sub>-NH<sub>2</sub> (**12**), backbone-modified analogues (**13–21**), and minimum growth inhibitory concentrations (MICs) against *E. coli* and MRSE

Peptide	Modification				MIC ( $\mu$ M)	
	R <sup>1</sup>	R <sup>2</sup>	R <sup>3</sup>	R <sup>4</sup>	<i>E. coli</i>	MRSE
<b>12</b>	H	H	H	H	50	12.5
<b>13</b>	H	H	H	NH <sub>2</sub>	50	12.5
<b>14</b>	H	H	NH <sub>2</sub>	NH <sub>2</sub>	50	25
<b>15</b>	H	NH <sub>2</sub>	NH <sub>2</sub>	NH <sub>2</sub>	25	12.5
<b>16</b>	NH <sub>2</sub>	NH <sub>2</sub>	NH <sub>2</sub>	NH <sub>2</sub>	25	6.25
<b>17</b>	H	H	H	Me	50	25
<b>18</b>	H	Me	Me	Me	200	200
<b>19</b>	H	Me	Me	Me	100	100
<b>20</b>	Me	Me	Me	Me	200	100
<b>21</b>	OH	OH	OH	OH	200	100

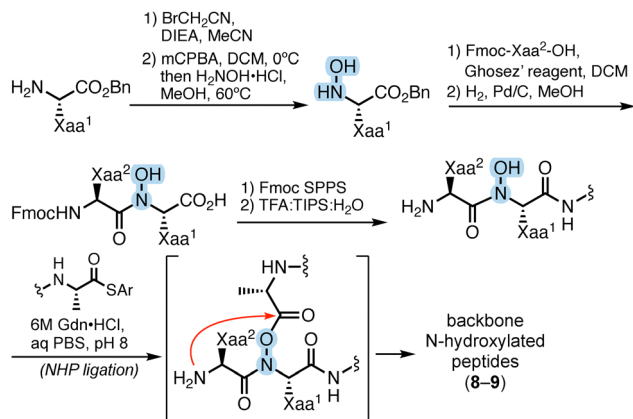


**Fig. 4** Synthesis of NHP variants **8** and **9** through hydroxamate-mediated peptide ligation.



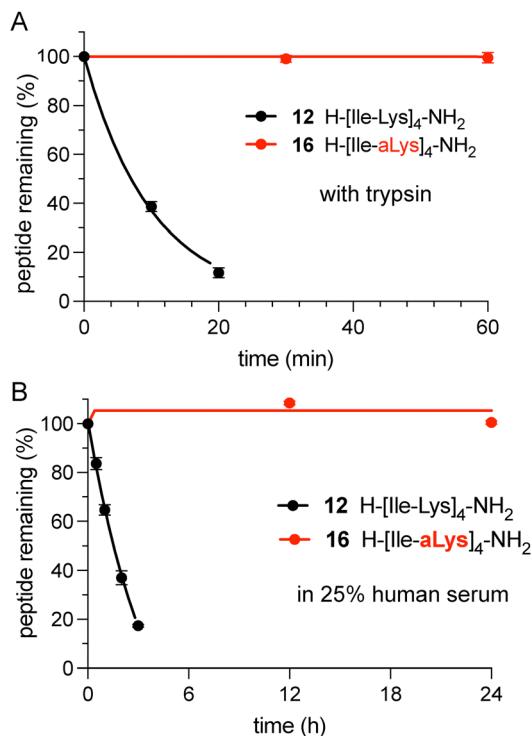


Fig. 6 (A) Stabilities of peptide **12** and tetra-NAP variant **16** against trypsin, and (B) in 25% human serum, monitored by RP-HPLC ( $\lambda = 220$  nm). Curves are derived from non-linear regression, and error bars represent SD for each data point ( $n = 3$ ).

of **12** would impart resistance to proteolysis while maintaining or reinforcing conformation-dependent antibacterial activity.

We prepared a series of *N*-aminated and *N*-methylated octapeptides in which one to four Lys residues were replaced with aLys or MeLys (**13–20**, Table 3). The growth inhibitory activity of these peptides was evaluated against *Escherichia coli* (*E. coli*) and methicillin-resistant *Staphylococcus epidermidis* (MRSE), as representative Gram-negative and Gram-positive pathogens, respectively. Minimum inhibitory concentrations (MICs) were determined using a standard microbroth dilution assay. The unmodified parent peptide **12** exhibited MIC values of 50  $\mu\text{M}$  against *E. coli* and 12.5  $\mu\text{M}$  against MRSE. Peptides **13–15**, containing one to three  $\alpha$ -hydrazino acid substitutions, displayed antibacterial activities comparable to that of peptide **12**, whereas tetra-*N*-aminated analogue **16** exhibited a two-fold enhancement in activity against both pathogens. Mono-NMP **17** exhibited similar antibacterial activity against both pathogens compared to the unmodified peptide **12**, while analogues **18–20**, containing two to four MeLys substitutions, exhibited significantly reduced activity. This result is consistent with a previous report showing that *N*-methylation of amphipathic  $\beta$ -sheet peptides significantly reduces their membrane lytic activity.<sup>28</sup> Encouraged by the antibacterial activity of tetra-NAP **16**, we synthesized a tetra-*N*-hydroxylated analogue (**21**) using a dipeptide building block approach. In contrast to **16**, tetra-NHP **21** exhibited significantly weaker activity against both pathogens relative to **12**.

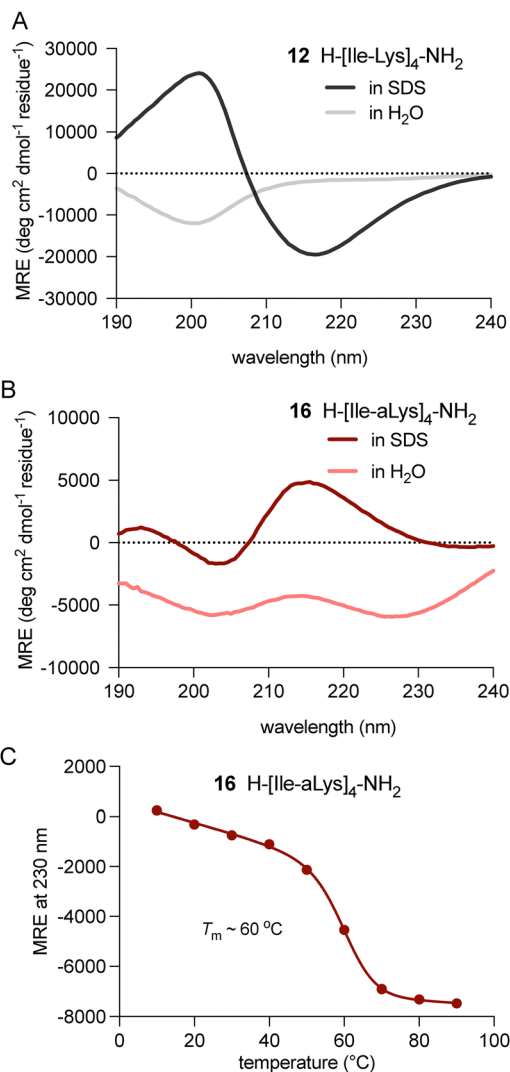


Fig. 7 Far-UV CD wavelength scans of (A) parent AMP **12** and (B) tetra-NAP variant **16**. Samples were analyzed at 0.5 mg mL<sup>-1</sup> in unbuffered water or 25 mM aq SDS. (C) Thermal denaturation of **16** in 25 mM aq SDS determined by VT CD, with fitted curve derived from non-linear regression.

Having identified **16** as the most potent inhibitor of bacterial growth, we evaluated its stability against trypsin and in human serum (37 °C) relative to the unmodified peptide **12**. The fraction of intact peptide over time was monitored by analytical LC-MS. As expected, peptide **12** was rapidly degraded by trypsin within 20 minutes. Conversely, analogue **16** remained completely intact over 24 hours under identical conditions (Fig. 6A and Fig. S3A). Similarly, **12** underwent near complete degradation within 3 hours in human serum, whereas tetra-NAP **16** remained fully intact over the course of 400 hours as determined by LC-MS (Fig. 6B and Fig. S3B). This result demonstrates that poly-*N*-amination can dramatically enhance peptide serum stability, particularly when employed at every other backbone amide. Moreover, the incorporation of one or more non-canonical  $\alpha$ -hydrazino acids into the parent octapeptide served to maintain or improve antibacterial activity in every



case, unlike *N*-methylation, which substantially reduced activity in most cases.

Finally, we assessed whether the antibacterial activity of peptide **16** is the result of altered secondary structure in a membrane environment. Circular dichroic (CD) spectra were thus obtained for peptides **12** and **16** in pure water and in the presence of 25 mM SDS as a membrane-mimicking surfactant. As previously reported, peptide **12** exhibited a random coil signature in water and a clear  $\beta$ -sheet structure in the presence of SDS, indicating environment-dependent folding (Fig. 7A).<sup>26</sup> In contrast, **16** displayed anomalous CD signatures in pure water and aq SDS (Fig. 7B). These spectra likely arise from perturbed electronic transitions, owing to the presence of four hydrazide bonds within the strand.<sup>29</sup> However, the clearly distinct signatures for **16** in water *versus* aq SDS are also indicative of environment-dependent adoption of secondary structure.

Interestingly, the CD spectrum of unmodified peptide **12** in aq SDS remained unchanged even at 90 °C, suggesting strong membrane association with a highly stable  $\beta$ -sheet-like structure (Fig. S4A). In contrast, thermal denaturation of peptide **16** in aq SDS revealed a well-defined isodichroic point indicative of cooperative unfolding (Fig. S4B). Fitting to a two-state denaturation model revealed a  $T_m$  of  $\sim 60$  °C (Fig. 7C).<sup>30</sup> Although the precise conformation of **16** in aq SDS is unknown, our results indicate that tetra-*N*-amination provides complete protection from degradation in serum while maintaining the ability to adopt a biologically active fold.

## Conclusions

Here, we systematically examined how backbone N-heteroatom substitution influences peptide proteolytic stability as a function of position relative to a defined cleavage site. *N*-Amination confers pronounced protection when introduced at the P1 and P1' positions of the chymotrypsin substrate, consistent with disruption of interactions required for protease recognition. Direct comparison with *N*-hydroxylation and *N*-methylation reveals that these backbone modifications exert distinct effects on proteolytic susceptibility, possibly reflecting differences in the electronic properties and H-bonding capacities of the modified amide bonds. Notably, *N*-amination at the scissile bond (P1') significantly enhances proteolytic stability despite the increased electrophilicity of the hydrazide carbonyl.

The protective effects of *N*-amination were extended to an amphipathic antimicrobial octapeptide whose biological activity is linked to its  $\beta$ -sheet-like structure. Poly-*N*-amination dramatically enhances serum stability while improving antibacterial activity, whereas poly-*N*-methylation reduces membrane lytic activity. Circular dichroism studies indicate that tetra-*N*-amination preserves the ability of the peptide to adopt a membrane-associated folded state despite an unnatural residue content of 50%.

Together, these results establish backbone N-heteroatom substitution as a chemically distinct and minimally perturbing

strategy for enhancing the proteolytic stability of bioactive peptides. In conjunction with their known conformational preferences, we anticipate that backbone *N*-amination and *N*-hydroxylation will find utility in the design of folded peptide and protein mimics for studies in cells and *in vivo*.

## Author contributions

A. F. A. and N. C.-S. conducted the experimental work. A. F. A., N. C.-S., and J. R. D. conceptualized the project, analyzed the data, and prepared the manuscript.

## Conflicts of interest

There are no conflicts to declare.

## Data availability

The data supporting this article have been included as part of the supplementary information (SI). Supplementary information is available. See DOI: <https://doi.org/10.1039/d6cb00061d>.

## Acknowledgements

This work was supported by a grant from the National Science Foundation (CHE2109008). We gratefully acknowledge fellowship support to A. F. A. from NIH grant T32GM145773, the Berthiaume Institute for Precision Health, and the Welter Family Foundation. We thank Prof. Yichun Wang for access to CD instrumentation. We thank Prof. Christian Melander and Dr Ansley Nemeth for providing materials and bacteria used to determine antibacterial activity.

## Notes and references

- 1 L. Nevola and E. Giralt, *Chem. Commun.*, 2015, **51**, 3302–3315.
- 2 L.-G. Milroy, T. N. Grossmann, S. Hennig, L. Brunsveld and C. Ottmann, *Chem. Rev.*, 2014, **114**, 4695–4748.
- 3 J. D. A. Tyndall, T. Nall and D. P. Fairlie, *Chem. Rev.*, 2005, **105**, 973–999.
- 4 K. Fosgerau and T. Hoffmann, *Drug Discovery Today*, 2015, **20**, 122–128.
- 5 X. Lai, J. Tang and M. E. H. ElSayed, *Expert Opin. Drug Discovery*, 2021, **16**, 1467–1482.
- 6 L. Gentilucci, R. De Marco and L. Cerisoli, *Curr. Pharm. Des.*, 2010, **16**, 3185–3203.
- 7 A. Bhat, L. R. Roberts and J. J. Dwyer, *Eur. J. Med. Chem.*, 2015, **94**, 471–479.
- 8 H. M. Werner, C. C. Cabalteja and W. S. Horne, *ChemBioChem*, 2016, **17**, 712–718.
- 9 M. Erak, K. Bellmann-Sickert, S. Els-Heindl and A. G. Beck-Sickinger, *Bioorg. Med. Chem.*, 2018, **26**, 2759–2765.
- 10 O. Al Musaimi, L. Lombardi, D. R. Williams and F. Albericio, *Pharmaceuticals*, 2022, **15**, 1283.



- 11 C. Lamers, *Future Drug Discovery*, 2022, **4**(2), FDD75, DOI: [10.4155/fdd-2022-0005](https://doi.org/10.4155/fdd-2022-0005).
- 12 J. Chatterjee, C. Gilon, A. Hoffman and H. Kessler, *Acc. Chem. Res.*, 2008, **41**, 1331–1342.
- 13 S. V. Fiacco and R. W. Roberts, *ChemBioChem*, 2008, **9**, 2200–2203.
- 14 J. Chatterjee, F. Rechenmacher and H. Kessler, *Angew. Chem., Int. Ed.*, 2013, **52**, 254–269.
- 15 Y. C. Koay, N. L. Richardson, S. S. Zaiter, J. Kho, S. Y. Nguyen, D. H. Tran, K. W. Lee, L. K. Buckton and S. R. McAlpine, *ChemMedChem*, 2016, **11**, 881–892.
- 16 H. Ogawa, G. T. Burke, J. D. Chanley and P. G. Katsoyannis, *Int. J. Pept. Protein Res.*, 1987, **30**, 460–473.
- 17 S. Sagan, P. Karoyan, O. Lequin, G. Chassaing and S. Lavielle, *Curr. Med. Chem.*, 2004, **11**, 2799–2822.
- 18 M. P. Sarnowski, C. W. Kang, Y. M. Elbatrawi, L. Wojtas and J. R. Del Valle, *Angew. Chem., Int. Ed.*, 2017, **56**, 2083–2086.
- 19 M. P. Sarnowski, K. P. Pedretty, N. Giddings, H. L. Woodcock and J. R. Del Valle, *Bioorg. Med. Chem.*, 2018, **26**, 1162–1166.
- 20 M. P. Sarnowski and J. R. Del Valle, *Org. Biomol. Chem.*, 2020, **18**, 3690–3696.
- 21 S. K. Starnes, W. S. Horne and J. R. Del Valle, *J. Org. Chem.*, 2025, **90**, 17214–17220.
- 22 I. J. Angera, M. M. Wright and J. R. Del Valle, *Acc. Chem. Res.*, 2024, **57**, 1287–1297.
- 23 A. F. Anwar and J. R. Del Valle, *J. Org. Chem.*, 2025, **90**, 6084–6089.
- 24 A. Armstrong, L. H. Jones, J. D. Knight and R. D. Kelsey, *Org. Lett.*, 2005, **7**, 713–716.
- 25 N. Cano-Sampaio and J. R. Del Valle, *Chem. – Eur. J.*, 2026, e70850.
- 26 Z. Y. Ong, S. J. Gao and Y. Y. Yang, *Adv. Funct. Mater.*, 2013, **23**, 3682–3692.
- 27 Z. Y. Ong, J. Cheng, Y. Huang, K. Xu, Z. Ji, W. Fan and Y. Y. Yang, *Biomaterials*, 2014, **35**, 1315–1325.
- 28 S. E. Miller, K. Tsuji, R. P. M. Abrams, T. R. Burke Jr and J. P. Schneider, *J. Am. Chem. Soc.*, 2020, **142**, 19950–19955.
- 29 M. M. Wright, B. H. Rajewski, T. A. Gerrein, Z. Xu, L. J. Smith, W. Seth Horne and J. R. Del Valle, *Commun. Chem.*, 2025, **8**, 76.
- 30 D. Shortle, A. K. Meeker and E. Freire, *Biochemistry*, 1988, **27**, 4761–4768.

